

# Analysis of dimple textured surfaces on cutting tools

Rodrigo L. Stoeterau<sup>1</sup> · Andreas Janssen<sup>2</sup> · Guilherme Mallmann<sup>2</sup>

Received: 23 October 2015 / Accepted: 25 November 2016 / Published online: 8 December 2016  
© The Brazilian Society of Mechanical Sciences and Engineering 2016

**Abstract** This paper presents the exploratory study of dimple-structured surfaces on cutting tools to reduce the friction between chip and the tool rake face. The objective is to study the effects of dimple-structured surfaces to the interactions between the chip and structured tool. Carbide inserts rake face which was structured with hemi-spherical micro-dimples with two different patterns using ultra-short pulse laser. Machining experiments were performed using three different materials: medium carbon grade steel ANSI 1045, cast iron ANSI GGG40, and aluminum alloy ANSI 2024-T6. The experiments were performed, under different cutting speeds and feed rates, at a constant cutting depth, and using 10% cutting fluid emulsion. Reference experiments were conducted with non-structured tool, and the results were compared. The results show that the interactions between the chip and structured rake face depend on the chip formation. Continuous chips with high contact length can produce enough lift hydrodynamic force to induce a cutting force reduction. No significance reduction on the cutting forces was observed for lamellar-segmented and discontinuous chips. The cutting parameters and the concentration of dimples are also importance design factor to be considered.

**Keywords** Machining · Dimples · Structured surfaces · Cutting tools

## 1 Introduction

The motivation of this investigation is the reduction of energy consumption and improvement of cutting tool wear resistance by geometry-based tribological approach by reduction of energy loss at the rake surface. The specific objectives are the understanding of micro-dimple distribution over the cutting force, and how the dimples act under different cutting parameters. The cutting force,  $F_c$ , was used as output control variable, because it is the major machining force component that acts on the rake face of the tool. Usually, the cutting force is the largest of the three machining force components and it is the main responsible for controlling the friction. For this investigation, carbides insert tools for turning, which had their rake face structured with micro-hemi-spherical dimples with two different distribution patterns, one providing high and other lower density of dimples.

Machining experiments were performed using three different materials: normalized medium carbon grade steel ANSI 1045 (hardness HV = 192), cast iron ANSI GGG40 (hardness HV = 182), and aluminum alloy ANSI 2024 (hardness HV = 126). The experiments were performed, under different cutting speeds and feed rates, at a constant cutting depth, and using 10% cutting fluid emulsion. Reference experiments were conducted with non-structured tool, and the results were compared. The results show that continuous chips with high contact length produces a better interaction with the dimple structured; this generates enough lift hydrodynamic force to induce a cutting force reduction. No significance reduction on the cutting forces

---

Technical Editor: Márcio Bacci da Silva.

✉ Rodrigo L. Stoeterau  
rlstoeterau@googlemail.com

<sup>1</sup> Department of Mechatronic Engineering and Mechanical Systems, University of São Paulo, São Paulo, Brazil

<sup>2</sup> Fraunhofer Institute for Production Technology, Aachen, Germany

was observed for lamellar-segmented and discontinuous chips. The cutting speed also has a strong influence over the results; no significant reduction on the cutting force was observed for low and high cutting speeds. This suggests that there is an optimum range of cutting speed, where the dimples can produce hydrodynamic lift. The concentration of dimples is also an important design factor to be considered.

Hamilton [1] describes the effects of surface micro-irregularities and cavities over the lubrication of parallel surface with motion. Hamilton concludes that lubrication mechanism depends on the asperity distribution, it is proportional to the velocity, and the structured asperities contribute to improve the load capacity. Etsion [2] explores the potential of micro-structured surfaces to improve tribological properties on reciprocating automotive components. Etsion [2] concludes that surface micro-texturing can efficiently be used to maintain hydrodynamic effects even with nominally parallel surfaces. It is also shown that optimum surface texturing may substantially reduce the friction losses in reciprocating automotive components. Etsion [3] developed an analytical model to predict the relation between the opening force and operating conditions in a mechanical seal with laser-structured surface with micro-dimples. Hamilton [1] and Etsion [2, 3] describe the effectiveness of surface textures in friction reduction for conformal contacts under high-speed and low-load applications. Hsu [4] explored the sliding problem of dimple-structured surfaces operating with higher contact pressures under lower speeds. Kovalchenko [5] investigated how a Laser Surface Texturing (LST) acts over the lubrication regimes and friction transitions on the Stribeck curve. The results show that laser texturing expanded the contact parameters in terms of load and speed for hydrodynamic lubrication, as indicated by friction transitions at the Stribeck curve. Yagi [6] describes how the introduction of micro-pits on surfaces under reciprocating movement improves the lubrication performance. Yagi [6] had a special focus on the arrangement of the micro-pits and concluded that the micro-pits of the same diameter, depth, and area density provide different friction coefficients depending on their arrangement. The difference in friction coefficient between the two arrangements sometimes achieves greater than twice. Stoeterau [7] conducted experiments with dimple-structured surfaces under no lubrication and observed that dimples can act as debris trap, reducing the wear by avoiding a three body contact.

## 2 The tribological problem chip/rake face problem

The chip formation during the cutting depends on the part material, tool material and part and tool geometry, process,

machining strategy, type and form of application of the cutting fluid, and cutting parameters (cutting speed— $v_c$ , feed rate— $f$ , and depth of cut— $a_p$ ). From the tribological point of view, the sliding contact among the inner surface of the chip and the tool face is an interesting and complex problem. At this interface, it is possible to observe that all the conditions of the Stribeck curve are present, from the dry friction to the hydrodynamic lubrication, depending on the chip formation conditions. During the chip formation at region near the cutting edge, there is no condition for the cutting fluid acts, due to contact pressure resulting from the deformation process at the chip root; at this point, we can observe dry friction. As the chip slides continue the contact area between the chip inner surface and the tool rake face increase, decreasing the contact pressure, which associated with the surfaces roughness, starts to create conditions for a transition from dry friction to mix and elastohydrodynamic lubrication. At the point where the chip separation from the rake face, a full development of a hydrodynamic film can be observed. Figure 1 presents a generalized view for the contact tribological problem in the chip/tool face interface and its relation with the Stribeck curve.

The contact problem of chip/rake face in the machining with geometrically defined tools can be described as tribological systems that work under high contact pressure and high velocity, usually with low viscosity cutting fluids. For this reason, this paper explores the tribological problem of chip/rake face structured with dimples, with the objective of studying the interactions contact between the chip and tool rake face over the machining forces.

## 3 Dimple-structured tool design and manufacturing

The design of structured tool surfaces can be done using different types of shape, size, and distribution patterns. This allows the control of the friction and wear on parts with relative movement. For this investigation, the rake face of cutting tools was structured with hemi-spherical shape dimples with a diameter of 100 and 25  $\mu\text{m}$  deep. The hemi-spherical is the most used shape for dimples; the design and the pattern used follow the recommendations of Hamilton [1], Wang [8], Etsion [15], and Yu [9]. The dimples were arranged in a triangular pattern, and the distance between dimple centers ( $D_{\text{dimple}}$ ) defines the distribution pattern and the density of dimples per area unit, Fig. 2. Two distances between dimple centers were set for the experiments, 110 and 350  $\mu\text{m}$ , the first one gives a density of 100 dimples/ $\text{mm}^2$  and a reduction on the apparent support area of 3.9/ $\text{mm}^2$  and the second one gives a density of 13 dimples/ $\text{mm}^2$  and a reduction on the apparent support area of 1.1/ $\text{mm}^2$ . The distribution pattern allows the control over the

**Fig. 1** Generalized view for the tribological contact problem in the chip/tool rake face interface

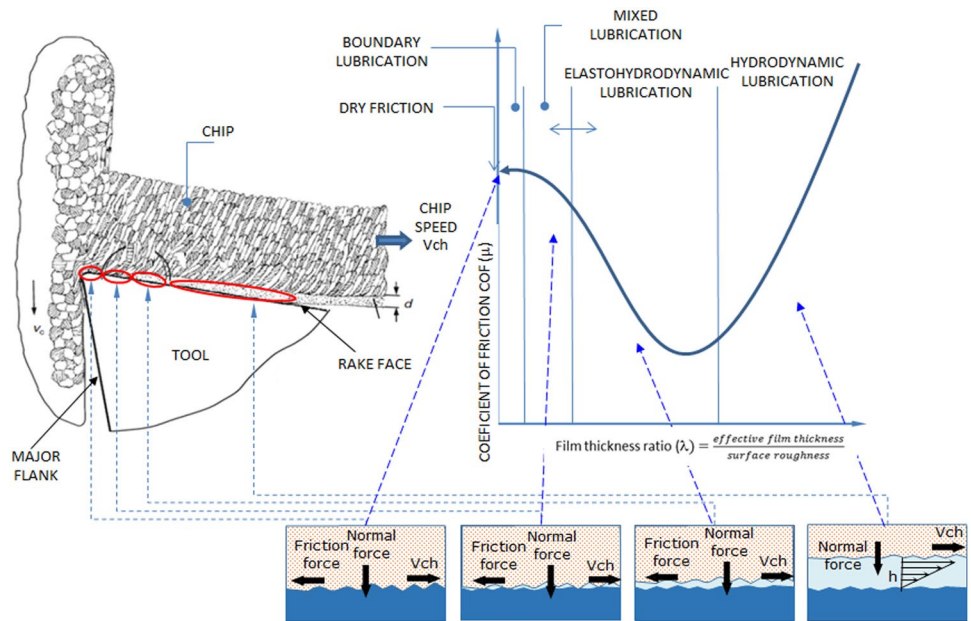
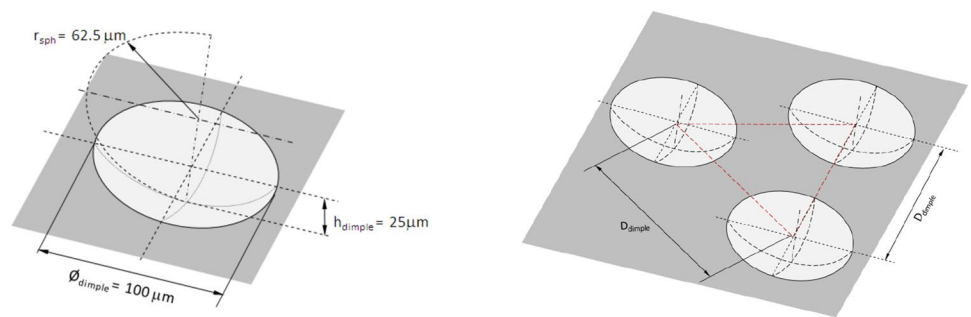


**Fig. 2** Design of the dimples and the distribution pattern



apparent area of support and the effect of the dimples density over the friction at the interface.

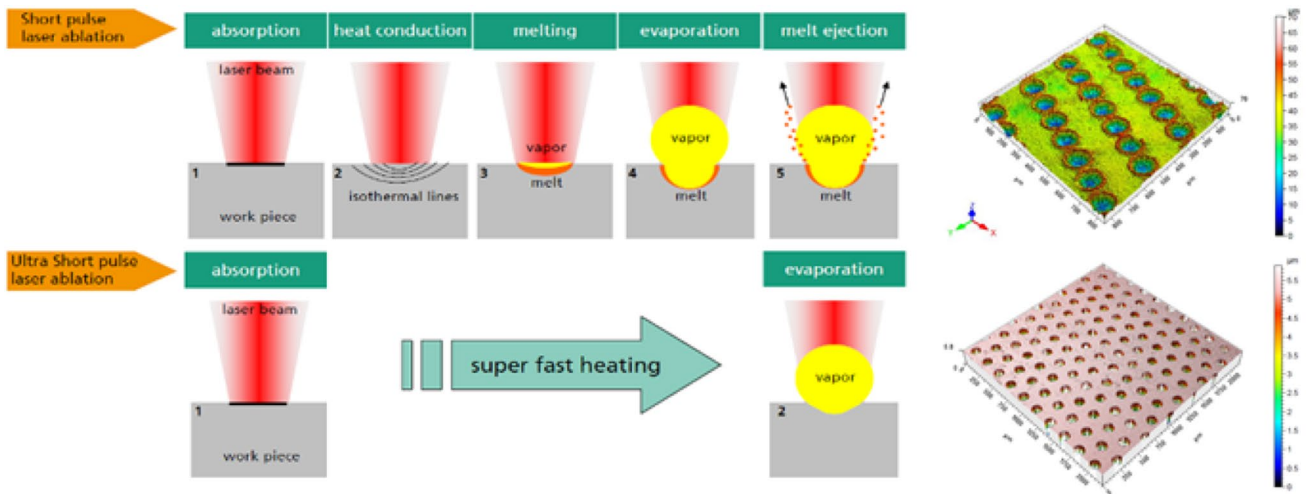
The dimples were manufactured using a pulsed laser ablation with an ultra-short pulse (usp) laser. The main characteristic of usp laser ablation is the thermal appearance of the material evaporation, without a liquid phase, which facilitates the manufacturing of surface micro-structures with accurate geometries on scale of several micrometers. Figure 3 illustrates the fundamental principle for the two main principles laser ablation: the short pulse (sp) laser and ultra-short pulse (usp) laser, and it brings a comparative resulting form for dimples obtained with the two process [10]. The short pulse laser allowed the solidification of part material ablated allowing a burr formation on the border of the dimple [10, 11]. The dimple border burr changed its geometry and the chip/rake face contact conditions. The difference between the two principles origins from the duration of the laser pulses and results in different ablation properties and thermal damages [12].

The ratio of occurrence for each effect depends on many quantities regarding the laser process as well as the

operational parameters of the tribosystems. While the laser process parameters define the possibilities of the manufacturing process for micro-structures, the operational conditions define kind and geometric specifications of micro-structures to be finished.

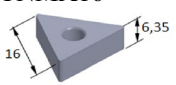
A Kern Evo (5-axis) *Pikosekunden-Laserstrahlstrukturiersystem* using a Laser source Lumera Super-Rapid, with an average output power of 18 W at 1 MHz, wavelength: 1064 nm/532 nm, repetition rate from 80 kHz to 1 MHz [22], and a focal point of 0,5  $\mu\text{m}$ . The machining parameters used on the dimples manufacturing were: power: 7 W, pulse frequency; 100 kHz, speed: 60 mm/s; repetitions: 1X, burst mode pulsewidth lower than 15 ps.

The tool select for dimple texturization was a tungsten carbide K-20 TNMA16; Table 1 brings its main geometrical characteristics. A negative rake angle ( $\gamma_0 = -6^\circ$ ) tool was chosen; in spite of not recommended for aluminum alloys, a negative rake angle is suitable for use with medium/high-strength steel, such as ANSI 1045, or grey cast iron. To preserve the cutting edge 0–2 mm, a retreat was done until the first row of dimples. Previous experiments performed prior



**Fig. 3** Physical mechanisms of pulsed laser ablation, short pulse, and ultra-short pulse

**Table 1** Tool characterization

Tool Type	TNMA16 	Shape: Triangular 60° Relief Angle $\alpha$ : 0° Tolerance: 0.05 to 0.13mm	Central hole cylindrical Chip break: No Thickness: 6.35mm
Tool material	Tungsten Carbide P-35	Hardness HV = 1327	
Tool geometry	$\chi_r = 60^\circ$ $\lambda_n = -5^\circ$	$\varepsilon = 60^\circ$ $\alpha_n = 2^\circ$	$r_\varepsilon = 0.2 \text{ mm}$ $\gamma_0 = -6^\circ$

the final design shown the structuration near or at the cutting edge turn the tool easily to the collapse. The dimples were manufactured in a 1–7 mm wide row, this covers most of rake face surface, and this allows experiments at high feed rates with materials which produces ribbon chips, such as low carbon steels, some aluminum alloys, and polymers. Table 2 shows the tool design specifications and characterization post-dimple manufacturing.

### 4 Experimental procedure

The part materials selected for the experiments were a medium carbon steel ANSI 1045, which produces lamellar-segmented chips, aluminum ANSI 2024, which produces continuous chips, and cast iron GGG40 which produces discontinuous chip, characteristic of fragile material [13].

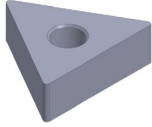
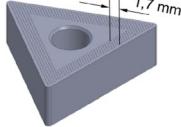
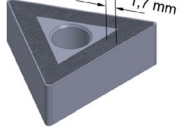
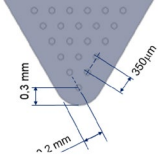
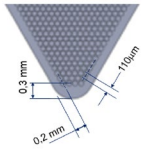
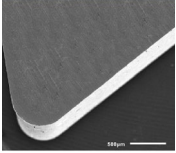
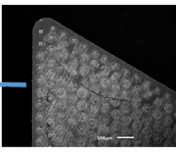
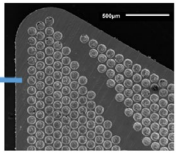
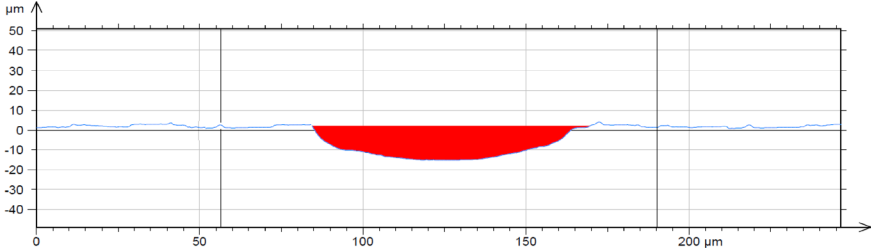
The cutting parameters for each material are at Table 3, and the experiments were performed at a constant cutting depth, using 10% emulsion as a cutting fluid. Five repetitions were performed for each cutting condition, each one with a new cutting edge. The graphics represents the

average of the five experiment replications, and the statistical error is associated with each one. A *T* test with significance of 98% was done to verify if the differences observed are significant or not.

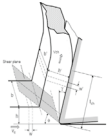
The tool–chip contact length, Fig. 4, determines major tribological conditions at tool/chip interface as temperatures, stresses, tool wear, etc. This length is found to be very sensitive to any change in the parameters and characteristics of the cutting process. Depending on its magnitude, the dimple affects can be barely or non-sensitive. The relation between the cutting parameters and the contact length is important, because the optimization of tribological processes at the tool–chip interface can be accomplished only when these correlations are known and well understood.  $\bar{l}_{ch}$ , at Table 3, represents the average tool–chip contact length, measured experimentally. Figure 4 also brings the equations to calculate  $\bar{l}_{ch}$  base on the geometrical characteristics of the orthogonal cut according to Altintas [14].

The experiments were conduct using a Monfort lathe UniCen 700, and Fig. 5 shows a general view of the experiments. All the experiments were conducted using cutting fluid that was emulsion 10%.

**Table 2** Tool design and characterization

Reference tools	Ddimples = 350 $\mu\text{m}$	Ddimples = 110 $\mu\text{m}$
		
		
Cutting edge retreat (CEr)	<b>0.2 mm</b>	<b>0.2 mm</b>
		
Average dimple profile		

**Table 3** Cutting parameters for the experiments

	Aluminum ANSI 2024			Carbon steel ANSI 1045			Cast iron GGG40			
Cutting speed [m/min]	150	350	500	90	140	220	100	250		
Feed rate [mm/rev]	0.1	0.25	0.4	0.1	0.35	0.6	0.12	0.35	0.5	
Cutting depth - $a_p$ [mm]	1.2			1.2			1.2			
	b [mm]	1.39			1.39			1.39		
	h [mm]	0.0866	0.2165	0.3464	0.0866	0.3031	0.5196	0.1039	0.3031	0.8660
	$\bar{l}_{ch}$ [mm]	0.18	0.43	0.90	0.19	0.52	1.20	0.22	1.34	4.81

**5 Experimental results and analysis**

The cutting force,  $F_c$ , is the component of the force acting on the rake face of the tool, and it is the main responsible for controlling the friction force. This is usually the largest of the three force components and acts in the direction of the cutting velocity. Statistical analysis  $T$  test with 98% of significance was performed to support the conclusions. The analysis was done considering the effects of the

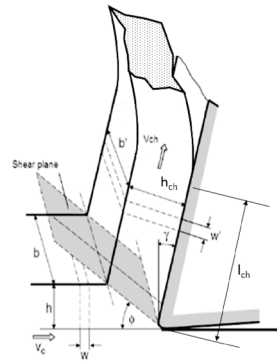
hydrodynamic lift force from the dimples, over the cutting force.

Figure 6 shows the comparative results for the machining forces for turning of Aluminum ANSI 2024, for non-structured tool ( $D_{\text{dimples}} = 0$ ) and structured tool with high concentration of dimples ( $D_{\text{dimples}} = 110\mu\text{m}$ ) and low concentration ( $D_{\text{dimples}} = 350\mu\text{m}$ ).

Based on Fig. 6, at a cutting speed of 150 m/min and feed rate of 0,1 mm/rev, the average  $\bar{l}_{ch}$  is 0.18 mm, and



**Fig. 4** Contact length definition on orthogonal cutting



$$l_{ch} = \frac{h \cdot \sin(\phi + \beta_f - \gamma)}{\sin\phi \cdot \cos\beta_f} \tag{Eq. 1}$$

$$\phi = \arctan\left(\frac{r_c \cos\gamma}{1 - r_c \cdot \sin\gamma}\right) \tag{Eq. 2}$$

$$\lambda_h = \frac{h}{h_{ch}} \tag{Eq. 3}$$

$$\beta_f = \lambda + \arctan\left(\frac{F_f}{F_c}\right) \tag{Eq. 4}$$

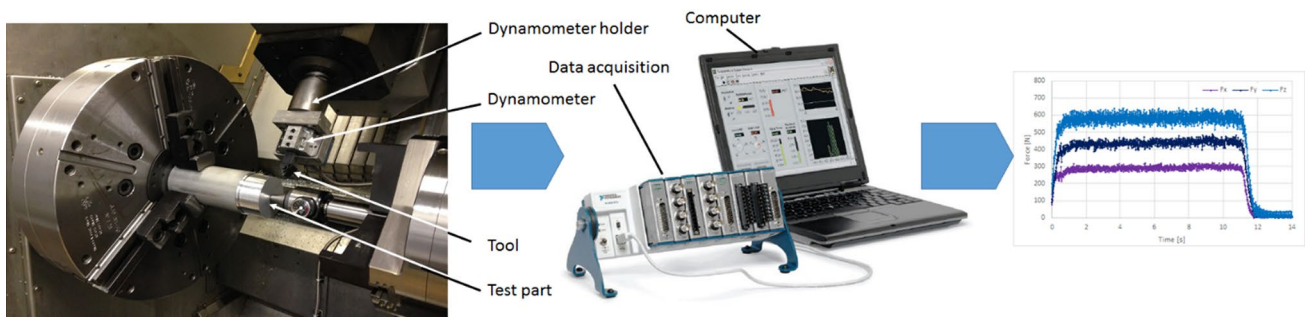


**Fig. 5** Experimental apparatus

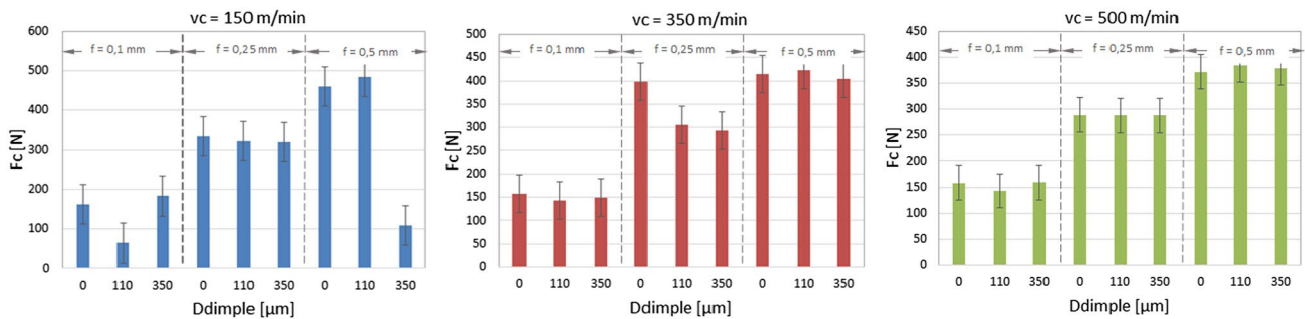


**Fig. 6** Cutting force analyses for Aluminum ANSI 2024

it is smaller than the cutting edge retreat (0.2 mm) and the effects of the dimples can be barely. The dimples presence cannot explain the reduction over the cutting force measure with tool with Ddimple 110 μm. The same conclusion can be extended for cutting speeds of 350 and 500 m/min.

For a feed rate of 0.25 mm/rev at a cutting speed of 150 m/min,  $\bar{l}_{ch}$  of 0.43 mm, the presence of dimple in any concentration produces a non-significance decrease at the cutting force. For a cutting speed of 350 m/min, a reduction on the cutting force is observed, and the presence of dimples produces no effect over the cutting force for a cutting speed of 500 m/min.

For a feed rate of 0.5 mm/rev at a cutting speed of 150 m/min, with  $\bar{l}_{ch}$  of 0.9 mm, only a high concentration

of dimples (Ddimple = 110 μm) produces a significant reduction over the cutting force. For cutting speed of 350 and 500 m/min, no gain was observed.

Figure 7 shows the comparative results for the cutting force for the turning medium carbon steel ANSI 1045, for non-structured tool and structured tool with high concentration of dimples (Ddimples = 110μm) and low concentration (Ddimples = 350μm).

For a cutting speed of 90 m/min, feed rate of 0–1 mm/rev, and  $\bar{l}_{ch}$  of 0.19 mm, the separation chip/tool at the rake face occurs near the dimples belt, and the effects of the dimples can be barely or none. The same conclusion can be extended for cutting speeds of 140 and 240 m/min. The experiments performed at a cutting speed of 90, 140,

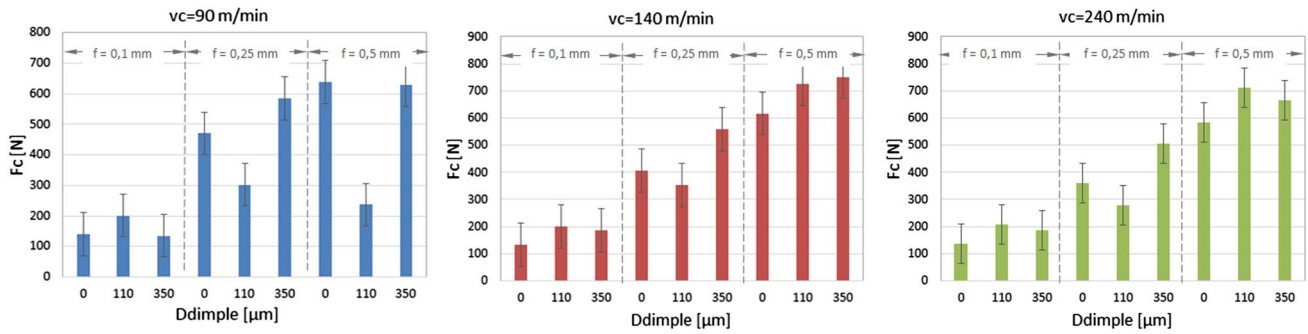


Fig. 7 Cutting force analyses for medium carbon steel ANSI 1045

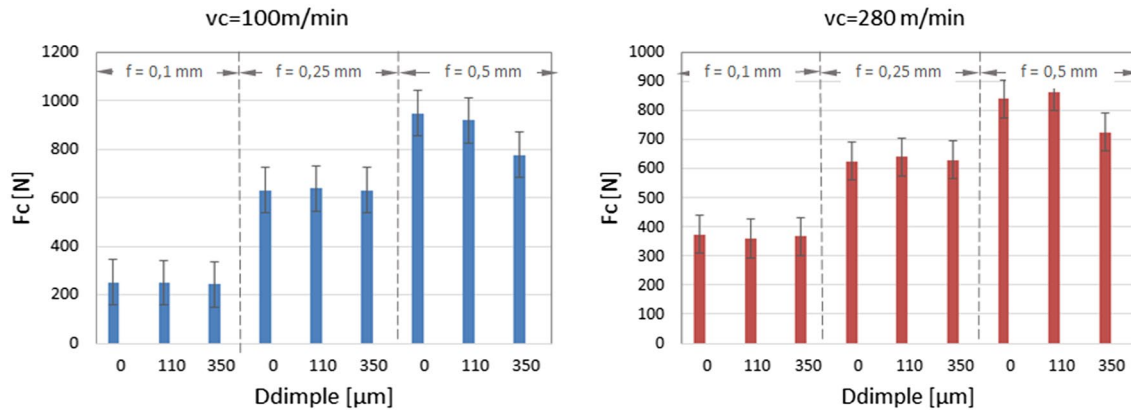


Fig. 8 Cutting force analyses for grey cast iron ANSI GGG40

and 240 m/min and feed rate of 0.25 m/rev; a significant decrease at the cutting force is observed only for a high concentration of dimples ( $D_{dimples} = 110 \mu\text{m}$ ). For the same cutting speeds at feed rate of 0.5 mm/rev, a significant reduction at the cutting force was observed only for a high concentration of dimples ( $D_{dimples} = 110\mu\text{m}$ ).

Figure 8 shows the comparative results for the cutting force for the turning of cast iron GGG400 for non-structured tool and structured tool with high concentration of dimples ( $D_{dimples} = 110 \mu\text{m}$ ) and low concentration ( $D_{dimples} = 350 \mu\text{m}$ ).

Based on Fig. 8, it is possible to observe for a cutting speed of 100 and 280 m/min, a marginal gain is obtained only at a feed rate of 0.5 mm/rev, with a low concentration of dimples ( $D_{dimples} = 350\mu\text{m}$ ).

### 6 Conclusions

The use of dimples structured cutting tool is very sensible to the part material, which under normal cutting conditions defines the chip type.

Aluminum ANSI 2024 produces continuous chips, under low cutting speed ( $v_c = 150 \text{ m/min}$ ); a low concentration of dimples could produce a cutting force reduction at high feed rate ( $f = 0.5 \text{ mm/rev}$ ). For intermediate cutting speed ( $v_c = 350 \text{ m/min}$ ), operating at a feed rate of 0.25 mm/rev, the presence of a dimple structure at low and high concentration was able to produce a consistent reduction over the cutting force. Under these conditions ( $v_c = 250 \text{ m/min}$ ,  $f = 0.25 \text{ mm/rev}$ ), no significant difference over the cutting force was observed between a high and low concentration. When operating at high cutting speed ( $v_c = 500 \text{ m/min}$ ), no reduction was obtained for any feed rate.

For medium carbon steel ANSI 1045, which produces lamellar-segmented chips, the presences of dimples produce better results. For a cutting speed of 90 m/min, a high concentration of dimples was able to reduce the cutting forces when operating under feed rates of 0.25 and 0.50 mm/rev. At a cutting speed of 140 and 240 m/min, a reduction was obtained only for a high concentration of dimples at a feed rate of 0.25. For the same cutting speeds operating at high feed rate ( $f = 0.5 \text{ mm/rev}$ ), no gain was observed.

Grey cast iron ANSI GGG40, which produces discontinuous chip, and characteristic of fragile materials, even with large contact length, are not able to produce enough hydrodynamic lift force at the dimples to produce a reduction of the friction force at the chip/rake face, decreasing the cutting force.

For the design of dimple-structured surfaces studied, a better results depend on the chip formation, chip rake face contact length, the dimples concentration, and the cutting parameters. For Aluminum ANSI 2024 and medium carbon steel ANSI 1045, non-fragile materials, when operating at high cutting speed and feed rate, the use of dimple-structured surfaces brings no effect over the cutting force. The same was observed at low feed rates at any cutting speed; at this condition, the chip contact length was not high enough to enter into the structured belt.

**Acknowledgements** The author would like to thank the *Comissão de Aperfeiçoamento de Pessoal de Nível Superior* (CAPES-Brazil) and Deutsche Forschungsgemeinschaft (DFG Germany), and the Brazil Germany program on advanced manufacturing (Bragecgrim) for supporting this research.

## References

- Hamilton DB, Walowit JA, Allen CMA (1996) Theory of lubrication by microirregularities. *J Fluids Eng* 88(1):177–185. doi:[10.1115/1.3645799](https://doi.org/10.1115/1.3645799)
- Ronen A, Izhak Etsion I, Kligerman Y (2001) Friction-reducing surface-texturing in reciprocating automotive components. *Tribol Trans*. doi:[10.1080/10402000108982468](https://doi.org/10.1080/10402000108982468)
- Etsion I, Halperin G (1999) Analytical and experimental investigation of laser-textured mechanical seal faces. *Tribology Transactions* 42(3)
- Hsu SM, Jing Y, Hua D, Zhang H (2014) Friction reduction using discrete surface textures: principle and design. *Journal of Physics D: Applied Physics*
- Kovalchenko A, Ajayi O, Erdemir A, Fenske G, Etsion I (2005) The effect of Laser surface texturing on transition in lubrication regimes during unidirectional sliding contact. *Tribol Int* 38:219–225
- Yagi K, Takedomi W, Tanaka H, Sugimura J (2008) Improvement of Lubrication Performance by Micro Pit Surfaces, *Tribology Online*, Tribology Conference Tokyo 2008
- Stoeterau RL, Sinatora A, Tertuliano I, Pavesi C, Fruchtingarten F, Ono FS (2014) Study of dimple texturized surfaces operating without lubrication. SAE international congress, São Paulo
- Wang X, Liu W, Zhou F, Zhu D (2009) Preliminary investigation of the effect of dimple size on friction in line contacts. *Tribol Int* 42:1118–1123
- Yu H, Huang W, Wang X (2013) Dimple patterns design for different circumstances. *Lubr Sci* 25:67–78. doi:[10.1002/lis.168](https://doi.org/10.1002/lis.168)
- Andrew Dunn A, Carstensen JV, Włodarczyk KL, Hansen EB, Gabzdyl J, Harrison PM, Shephard JD, Hand DP (2014) Nanosecond laser texturing for high friction applications. *Opt Lasers Eng* 62:9–16
- Nolte S, Momma C, Jacobs H, Tünnermann A (1997) Ablation of metals by ultrashort laser pulses. *J Opt Soc Am* 14(10):2716–2722
- Cichkov BN, Momma C, Nolte S, Von Alvensleben F, Tuennermann A (1996) Femtosecond picosecond and nanosecond laser ablation of solids. *Appl Phys A* 63:109–115
- Klocke F (2011) *Fertigungsverfahren 1: Drehen, Frasen, Bohren*, Springer-Verlag
- Altıntaş Y (2012) *Manufacturing automation—metal cutting mechanics, machine tool vibrations, and cnc design*, 2nd edition, Cambridge University Press
- Etsion I (2005) State of the art in laser surface texturing. *J Tribol Trans ASME* 127(1):248–253. doi:[10.1115/1.1828070](https://doi.org/10.1115/1.1828070)